ELSEVIER

Journal of Hydrology 214 (1999) 144–164

Journal of Hydrology

Modeling of non-isothermal multi-component reactive transport in field scale porous media flow systems

Tianfu Xu[a,1,*], Javier Samper[a], Carlos Ayora[b], Marisol Manzano[c], Emilio Custodio[c,2]

[a]*Escuela de Ingenieros de Caminos, Canales y Puertos, Universidad de La Coruña, Spain*
[b]*Instituto de Ciencias de la Tierra, CSIC, Barcelona, Spain*
[c]*Departamento de Ingeniería del Terreno, Universidad Politécnica de Cataluña, Barcelona, Spain*

Received 20 October 1997; received in revised form 6 November 1998; accepted 6 November 1998

Abstract

A general 2-D finite element multi-component reactive transport code, TRANQUI, was developed, using a sequential iteration approach (SIA). It is well suited to deal with complex real-world thermo-hydro-geochemical problems for single-phase variably water saturated porous media flow systems. The model considers a wide range of hydrological and thermodynamic as well as chemical processes such as aqueous complexation, acid-base, redox, mineral dissolution/precipitation, gas dissolution/ex-solution, ion exchange and adsorption via surface complexation. Under unsaturated conditions only water flow is considered, although gas pressures are allowed to vary in space in a depth-dependent manner specified by the user. In addition to the fully iterative sequential approach (SIA), a sequential non-iterative approach (SNIA), in which transport and chemistry are de-coupled, was implemented and tested. The accuracy and numerical performance of SIA and SNIA have been compared using several test cases. The accuracy of SNIA depends on space and time discretization as well as on the nature of the chemical reactions. The capability of the code to model a real case study in the field is illustrated by its application to the modeling of the hydrochemical evolution of the Llobregat Delta aquitard in northeastern Spain over the last 3500 years during when fresh-water flow from a lower aquifer displaced the native saline aquitard waters. Manzano and Custodio carried out a reactive transport model of this case study by using the PHREEQM code and considering water flow, aqueous complexation, cation exchange and calcite dissolution. Their results compare favorably well with measured porewater chemical data, except for some of the cations. Our code is not only able to reproduce the results of previous numerical models, but leads to computed concentrations which are closer to measured data mainly because our model takes into consideration redox processes in addition to the processes mentioned above. A number of sensitivity runs were performed with TRANQUI in order to analyze the effect of errors and uncertainties on cation selectivities.

Keywords: Reactive transport; Multi-component; Non-isothermal; Variably saturated media, Geochemistry; Llobregat delta

1. Introduction

The safety assessment of urban and industrial waste disposal, the study of groundwater pollution as well as the understanding of natural groundwater quality patterns require the use of modeling tools which are able to consider both the transport of dissolved species

* Corresponding author. Fax: 1-510-4865686; e-mail: E-mail: Tianfu_Xu@lbl.gov

[1] Present address: Mail Stop 90-1116, Lawrence Berkeley National Laboratory, 1 Cyclotron Road, Berkeley, CA 94720, USA.

[2] On leave to the Geological Survey of Spain, Madrid, Spain.

0022-1694/99/$ - see front matter
PII: S0022-1694(98)00283-2

as well as their complex interactions with the solid (or gas) phases. Two major numerical approaches were proposed to solve the coupled problem: (1) direct substitution approach (DSA) according to which chemical equations are directly substituted into the transport equations and (2) sequential iteration approach (SIA) in which the transport and chemical equations are solved separately in a sequential manner and following an iterative procedure. DSA leads to a system of coupled highly non-linear transport equations. This approach were used by, among others, Valocchi et al. (1981), Jennings et al., 1982, Miller and Benson (1983), Carnahan (1990), Steefel and Lasaga (1994) and White (1995). Its main advantage is high accuracy and quadratic rate of convergence. However, it is very demanding in terms of computing time and memory, which can seriously limit its use in large problems (Yeh and Tripathi, 1989). It may be difficult to apply to field scale 2- and 3-D problems. On the contrary, the sets of equations that are solved simultaneously in the SIA are much smaller than in the DSA, and therefore larger systems with larger sets of chemical species can be handled with SIA. The latter approach was used by many investigators such as Kirkner et al. (1984), Walsh et al. (1984), Cederberg et al. (1985), Liu and Narasimhan (1989), Nienhuis et al. (1991), Yeh and Tripathi (1991), Engesgaard and Kipp (1992), Samper et al., (1994), Lensing et al. (1994), Šimnek and Suarez (1994), Walter et al. (1994), Zysset et al. (1994), and Neretnieks et al. (1997). Walter et al. (1994) argue that in problems dealing entirely with local equilibrium reactions there is no need to iterate between the transport and chemical equations. We denote this approach, the sequential non-iterative approach (SNIA). As shown later, our results indicate that they may be right, especially in problems with mineral dissolution/precipitation reactions. We are not aware of any systematic comparison of SIA and SNIA and therefore Walter et al.'s claim may not hold for other types of chemical reactions. In this article we present a comparison of their performance and accuracy in several problems dealing with different types of local equilibrium chemical processes. Our results indicate that SNIA leads to a substantial saving of computing time compared to SIA while its accuracy is generally good, although very dependent on (1) space discretization, (2) time increment size, and (3) nature of chemical reactions. The largest discrepancies between SNIA and SIA are observed in problems dealing with cation exchange which were not analyzed by Walter et al. (1994).

To cope with the need of general-purpose numerically efficient codes that can handle simultaneously the most relevant hydrodynamic, thermal and chemical processes in complex field-scale problems, here we present a 2-D finite element multi-component reactive transport code, TRANQUI, which can use either SIA or SNIA for the purpose of improving numerical efficiency. General water flow, heat transfer and solute transport boundary conditions are considered under fully or variably saturated conditions. The code accounts for a wide range of chemical processes such as aqueous complexation, acid–base, redox, mineral dissolution/precipitation, gas dissolution/exsolution, cation exchange and adsorption via surface complexation.

When analyzing water flow through partly saturated porous media, usually the role of the gas phase can be disregarded by assuming the gas phase to be immobile. According to de Marsily (1986), using the mobile air phase approach does not give results significantly different from the immobile approach, except for very special cases. TRANQUI is based on the immobile air approach. This means that for the purpose of solving the water flow, the whole gas phase is at the same pressure (usually the atmospheric pressure). In some cases, the partial pressure of a gaseous species may increase because of gas generation processes (such as CO_2 production in soils) while the total pressure of the gas phase may remain almost constant. To account for these conditions, TRANQUI allows partial pressures of gaseous species to vary in space in a depth-dependent manner specified by the user. TRANQUI uses thermodynamic and hydrochemical data contained in modified versions of the EQ3/6 chemical databases (Wolery, 1992).

TRANQUI was applied to synthetic and real problems (Xu, 1996). Here we report its application to the modeling of the hydrochemical evolution of the Llobregat Delta aquitard in northeastern Spain over the last 3500 years during which upwards fresh-water flow from a confined aquifer were displacing the native saline aquitard waters. Manzano and Custodio (1995) carried out a reactive transport model of this case study by using the PHREEQM code (Nienhuis et

al., 1991) and considering water flow, aqueous complexation, cation exchange and calcite dissolution. Their results compare favorably well with measured porewater chemical data, except for some of the cations. Our code is not only able to reproduce the results of previous numerical models, but leads to computed concentrations of some ions which agree better with measured data mainly because of the consideration of redox processes in addition to the previous processes. A number of sensitivity runs performed with TRANQUI illustrate the effect of uncertainties in cation selectivities on computed aqueous and exchanged concentrations.

2. Mathematical formulation

2.1. Water flow

By combining Darcy's Law with the mass balance equation, water flow in variably saturated media can be written as (Bear, 1979; Galarza, 1993; Šimnek and Suarez, 1994)

$$\nabla\cdot[K_r K \nabla(\psi + z)] + w = \left(\phi \frac{\partial S_w}{\partial \psi} + S_w S_s\right)\frac{\partial \psi}{\partial t}, \quad (1)$$

where ψ is pressure head, z is elevation, w is fluid source/sink per unit volume of medium, K is saturated hydraulic conductivity, K_r is relative conductivity (a function of pressure head; for fully saturated media $K_r = 1$), S_s is the specific elastic storage coefficient, ϕ is porosity, and S_w is water saturation defined as the ratio between the volumetric water content θ and porosity ϕ, or $S_w = \theta/\phi$ (for fully saturated media $S_w = 1$).

2.2. Heat transfer

Chemical parameters (activity coefficients, the dielectric constant of water and equilibrium constants) are generally functions of temperature. To account for the variation of these parameters with temperature one must know the temperature distribution. Temperature values can be obtained from solving the heat transport problem. The principle of heat conservation can be written as (de Marsily, 1986)

$$\nabla\cdot(\lambda \nabla T - \rho_w c_w q T) = \rho_m c_m \frac{\partial T}{\partial t}, \quad (2)$$

where λ is the thermal conductivity tensor, T is temperature, ρ_w is density of water, c_w is the specific heat of the water, ρ_m and c_m are density and specific heat of the bulk porous medium (water plus solid), and $\mathbf{q}$ is the Darcy velocity which can be calculated from solutions of the flow Eq. (1).

2.3. Multi-component reactive transport

Aqueous (dissolved) species are subject to transport in liquid phase as well as local chemical interactions with other aqueous species (homogenous reactions), and solid species (heterogeneous reactions). Solid species, including precipitated, exchanged and adsorbed surface species, only participate in local chemical reactions. In partly saturated media, gaseous species are subject to transport in the gas phase as well as reactions with aqueous species, which may strongly influence water chemistry. Although gas transport processes are not considered in the current version of our code, partial gas pressures are allowed to vary in space in a depth-dependent manner specified by the user.

For aqueous systems in chemical equilibrium, 'multi-species reactive transport' can be reduced to 'multi-component reactive transport' (Yeh and Tripathi, 1991; Walter et al., 1994; Steefel and Lasaga, 1994; Lichtner, 1996) if diffusion and dispersion coefficients can be assumed to be the same for all the aqueous species. Under these conditions, transport equations can be written in terms of total dissolved components. Based on mass conservation, transport equations for chemical components can be expressed as

$$\nabla\cdot(\theta D \nabla C_j) - q\cdot\nabla C_j + w(C_j^* - C) + \theta R_j = \theta\frac{\partial C_j}{\partial t} \quad (3)$$

$$j = 1, 2, \ldots, N_c,$$

where N_C is the number of chemical components, C_j is the total dissolved concentration of component j, C_j^* is the dissolved concentration of fluid sources of water flux w, $\mathbf{D}$ is the hydrodynamic dispersion tensor, and R_j is the reactive sink/source term which includes all the chemical interactions of the jth component with solid (or gas) species. In general, the chemical sink/source term depends on the concentrations of all dissolved species in a non-linear manner, which

renders the transport Eq. (3) highly non-linear. These primary governing equations need to be complemented with constitutive chemical relationships, which are local equations and express all secondary variables as functions of a set of primary variables.

2.4. Chemical reactions

For representing a geochemical system, it is convenient to select a subset of N_C aqueous species as basis species, which are the so-called components, or primary species by other authors. All non-primary species are called secondary species, which include aqueous complexes, precipitated (mineral) and gaseous species (Parkhurst et al., 1980; Yeh and Tripathi, 1991; Steefel and Lasaga, 1994; Lichtner, 1996). The number of secondary species must be equal to the number of reactions. All the secondary species can be represented as linear combinations of basis species such as

$$S_i^s = \sum_{j=1}^{N_c} v_{ij} S_j^p \qquad i = 1, \ldots, N_R, \tag{4}$$

where S_j^p is the chemical formula of the jth basis species, S_i^s is the chemical formula of the ith secondary species, N_R is the number of reactions (or secondary species), and v_{ij} is the stoichiometric coefficient of the jth basis species in the ith reaction.

Aqueous complexation. By assuming local equilibrium for aqueous complexation reactions, the mass action law provides an expression, which relates the concentration of the ith aqueous complex to the concentrations of basis species:

$$x_i = K_i^{-1} \gamma_i^{-1} \prod_{j=1}^{N_c} c_j^{v_{ij}^x} \gamma_j^{v_{ij}^x} \qquad i = 1, \ldots, N_x, \tag{5}$$

where N_x is the number of aqueous complexes, x_i are molal concentrations of aqueous complexes, c_j are molal concentrations of basis species, v_{ij}^x is the stoichiometric coefficient of the jth basis species in the ith aqueous complex, γ_i and γ_j are thermodynamic activity coefficients which can be calculated from available expressions such as that of Debye–Hückel, and K_i is the equilibrium constant.

Acid–base and redox reactions. Acid–base and redox reactions can be treated in a manner similar to aqueous complexation reactions (Yeh and Tripathi, 1989). Contrary to the proton, which exists as a dissolved species, the electron is a hypothetical species. Considering the electron as a dissolved species is convenient because it allows one to complete redox half-reactions such as $Fe^{2+} \Leftrightarrow Fe^{3+} + e^-$. A virtual concentration is attached to the electron, which by convention has an activity coefficient equal to 1. Consideration of redox reactions only requires an additional equation for the electron balance (''operational electrons'' according to Yeh and Tripathi, 1989).

Mineral dissolution/precipitation. The dissolution or precipitation of pure mineral phases under local equilibrium conditions is governed by the following expression

$$K_m = \prod_{j=1}^{N_c} c_j^{v_{mj}^p} \gamma_j^{v_{mj}^p} \qquad m = 1, \ldots, N_p, \tag{6}$$

where m is the mineral index, N_P is the number of minerals, v_{mj}^p is the stoichiometric coefficient of the jth basis species in the mth mineral, and K_m is the solubility constant.

Cation exchange. According to the Gaines–Thomas convention, cation exchange reactions can be written as (Appelo and Postma, 1993):

$$\frac{1}{z_i} S_i + \frac{1}{z_j}(S_j - X_{z_j}) \Leftrightarrow \frac{1}{z_i}(S_i - X_{z_i}) + \frac{1}{z_j} S_j, \tag{7}$$

where S_i and S_j denote dissolved cation species having electrical charges z_i and z_j, respectively, and $(S_i - X_{z_i})$ and $(S_j - X_{z_j})$ represent exchange sites occupied by exchanged cations. The equilibrium equation for cation exchange is obtained by applying the mass-action law to (7):

$$K_{S_i S_j} = \frac{\beta_i^{1/z_i} \cdot (\gamma_j c_j)^{1/z_j}}{\beta_j^{1/z_j} \cdot (\gamma_i c_i)^{1/z_i}}, \tag{8}$$

where $K_{S_i S_j}$ is the selectivity constant for cations S_i and S_j, and β_i and β_j are the activities of the exchanged cations which in the Gaines–Thomas convention are assumed to be equal to the equivalent fractions (Appelo and Postma, 1993). Any one of the cations can be taken as the reference cation. Here we take Na^+ as the reference cation. For a system with only three cations (Na^+, K^-, and Ca^{2-}), the exchange

reactions are written as:

$$Na^+ + K - X = K^+ + Na - X$$

$$Na^+ + 0.5Ca - X = 0.5Ca^{2+} + Na - X$$

and their selectivities are denoted by $K_{Na\,K}$ and $K_{Na\,Ca}$, respectively.

Our formulation and computer code accounts also for gas dissolution/ex-solution and adsorption via surface complexation using the double layer model. Interested readers will find details on these processes on the work of Xu (1996).

3. Numerical solution

3.1. Multicomponent reactive solute transport.

Our numerical formulation for solving the coupled equations of solute transport and chemical reactions is based on (Yeh and Tripathi, 1991; Walter et al., 1994) which consists on solving each set of equations separately in a sequential manner. One solves first the transport equations and then those of chemical reactions. This sequential process must be repeated several times until convergence is attained. The essence of the SIA is therefore the sequential solution of two independent sets of equations: the transport equations and the chemical equations. While the former is solved in a component manner, the latter must be solved nodewise. These two sets of equations are coupled by means of chemical sink/source terms. Yeh and Tripathi (1989) discuss the explicit and implicit schemes for SIA. The implicit scheme is more advantageous than the explicit because it is less prone to get negative concentrations, can be applied for obtaining steady-state solutions and shows a better convergence rate. The implicit scheme, however, requires using a transport operator slightly different than the standard transport operator. Our code uses a mixed explicit-implicit scheme based on the standard operator which enjoy adequate convergence properties (Samper et al., 1995; Xu, 1996). This scheme derives from rewriting Eq. (3) as

$$\nabla\cdot(\theta D\nabla C_j^{s+1/2}) - q\cdot\nabla C_j^{s+1/2} + w(C_j^* - C_j^{s+1/2}) + \theta R_j^s = \theta\frac{\partial C_j^{s+1/2}}{\partial t} j = 1,\ldots,N_c, \tag{9}$$

where superscript s denotes the transport + reaction iteration number. A transport + reaction iteration consists of two parts, a transport part denoted by s + 1/2 (it should be noted that 1/2 does not mean $\Delta t/2$ where Δt is the time step) and the reaction part denoted by s + 1. If the reaction sink/source term R_j^s in (9) are known, the resulting equations are linear and have the same structure as the standard transport equation of a conservative solute. These equations are solved by the Galerkin finite element method (Xu, 1996). After space and time discretization, the equation for the jth component becomes

$$\left[\varepsilon E + \frac{F}{\Delta t}\right]C_j^{k+1,s+1/2} = g_j^{k+1} + \theta R_j^{k+1,s} + \left[(\varepsilon - 1)E + \frac{F}{\Delta t}\right]C_j^k, \tag{10}$$

where ϵ is a time weighting parameter ($\epsilon = 0$ for explicit, $\epsilon = 1$ for implicit), **E** is a square matrix containing dispersion and advection terms. **F** is also a square matrix of storage terms, g_j^{k+1} is a column vector containing boundary terms as well as external fluid sink/source terms and superscript k denotes time step and $\Delta t = t^{k-1} - t^k$. The actual expressions of **E**, **F** and g_j^{k+1} are given by Xu (1996). The terms $R_j^{k+1,s}$ can be evaluated from the solution of the chemical equations are solved iteratively. In each iteration the reaction terms $R_j^{k+1,s}$ are updated until a specified convergence tolerance is satisfied. One should notice that the transport equations are solved on a component basis, whereas chemical equations are solved on a node basis. The SNIA is a particular case of SIA in which the sequence of transport and reaction equations is solved only once. Later in this article we analyze under what conditions the SNIA provides acceptably accurate solutions.

3.2. Solution of the reaction system

Our numerical formulation applies to problems with any type of homogeneous reactions (aqueous complexation, acid–base and redox) as well as any combination of heterogeneous reactions (mineral dissolution/precipitation, gas dissolution/exsolution, cation exchange and adsorption). For the sake of simplicity, out presentation here is restricted to problems with aqueous complexation and mineral dissolution/precipitation processes. Further details of these algorithms can be found in Xu (1996). The formulation is based on mass balances in terms of the basis species (Parkhurst et al., 1980; Yeh and Tripathi, 1991). The total analytical concentration of basis species, T_j, in the system are given by

$$T_j = c_j + \sum_{i=1}^{Nx} \nu_{ij}^x x_i + \sum_{i=1}^{Np} \nu_{ij}^p p_i \qquad j = 1,...,Nc, \quad (11)$$

where p_i is the ith mineral concentration and the first two terms of the right-hand side are total dissolved component concentrations, C_j

$$C_j = c_j + \sum_{i-1}^{Nx} \nu_{ij}^x x_i \qquad j = 1,...,Nc,$$

which are subject to transport (see Eqs. (3) and (9)). Here c_j denote the dissolved concentrations of primary species.

The set of non-linear chemical reactions is solved by the Newton–Raphson iterative method. The use of this method requires lumping all the terms in the right-hand side in a single term, which is denoted by F_j^c. After rearranging Eq. (11), one has;

$$F_j^c = c_j + \sum_{i=1}^{N_x} \nu_{ij}^x x_i + \sum_{i=1}^{N_p} \nu_{ij}^p p_i - T_j = 0 \quad j = 1,...,N_c. \quad (12)$$

Concentrations of the aqueous complexes, x_i are known functions of concentrations of the basis species, c_j (see Eq. (5)). No explicit expression relates the concentration of precipitated species, p_i, to c_j (Yeh and Tripathi, 1991). Therefore, N_p additional mass-action equations (one per mineral) are needed which are provided by Eq. (6). After rearranging these equations into a single term F_m^p, we obtain:

$$F_m^p = K_m^{-1} \prod_{j=1}^{Nc} C_j^{\nu_{mj}^p} \gamma_j^{\nu_{mj}^p} - 1 = 0 \qquad m = 1,...,Np. \quad (13)$$

These N_p equations plus the N_c equations in (12) provide the complete set of equations needed to solve for (N_c + N_p) unknowns (c_1, c_2,..., c_{Nc}, P_1, P_2,...,P_{Np}) which are lumped into a single vector of unknowns, X_i (i = 1, 2,...., N_c + N_p). In the Newton–Raphson method the unknowns are updated iteratively according to

$$X_i^{n+1} = X_i^n + \Delta X_i, \quad (14)$$

where n denotes the iteration number and ΔX_i are changes in unknowns, which are derived from the solution of the following set of linear equations

$$\sum_{i-1}^{N_c+N_p} \frac{\partial F_j}{\partial X_i} \Delta X_i = -F_j \qquad j = 1....,N_c + N_p, \quad (15)$$

which in matrix form reduces to

$$\mathbf{J}\Delta\mathbf{X} = -\mathbf{F},$$

where $\mathbf{J}$ is the Jacobian matrix, which contains the derivatives of the equations with respect to primary species, $\mathbf{F}$ is a column vector of residuals and $\Delta\mathbf{X}$ is the column vector of increments of unknowns. The evaluation of the Jacobian matrix is provided by Xu (1996). The iterative procedure is repeated until a specified convergence tolerance is satisfied.

Once the concentrations of the primary variables are obtained, all other secondary variables can be computed in a straightforward manner. The changes in mineral concentrations, Δ_{P_i}, are used to calculate the rate of mass transfer of component j from the mineral phase to the aqueous phase. The expression of the chemical sink/source term in Eq. (10) is computed as:

$$R_j = -\frac{1}{\Delta t} \sum_{i=1}^{N_p} \nu_{ij}^p \Delta p_i. \quad (16)$$

Notice that these sink/source terms may also have contributions from other heterogeneous reactions such as gas dissolution/ex-solution, cation exchange and surface adsorption. It should be pointed that chemical reactions are always solved per kg of

water (which is close enough to one litre of solution when its density is close 1 kg/l).

4. Numerical implementation

4.1. Solution steps and code capabilities

Based on this SIA (including SNIA), a two-dimensional finite element computer code, TRANQUI, was developed. At each time step, the coupled hydro-thermo-chemical system is solved by following these steps: (1) solution of the groundwater flow equation; (2) computation of groundwater velocities which are needed to evaluate solute and heat advective and dispersive terms; (3) solution of heat transport which is used to update temperature-dependent chemical parameters; (4) solution of multicomponent solute transport equations; and (5) solution of chemical reaction equations. Steps (4) and (5) must be repeatedly solved until some prescribed convergence criteria are satisfied.

Our code, TRANQUI, can be applied to general flow, solute transport and heat transfer conditions. It can cope with reactive transport problems having heterogeneous physical and hydrogeochemical properties in fully or partly saturated media. A wide range of chemical reactions, such as aqueous complexation, mineral dissolution/precipitation, gas dissolution/exsolution, cation exchange and surface complexation, are considered under local equilibrium assumptions. TRANQUI can take into account any number of species and reactions as long as they are contained in the attached chemical databases which at its current visions are constructed from modifications of EQ 3/6 databases (Wolery, 1992).

4.2. Convergence control

The solution of the non-linear reactive transport equations involve several iterative procedures. Each iterative procedure is performed until convergence is achieved. Convergence depends on several related factors such as: (1) the degree of non-linearity of the equations, (2) the initial concentrations at which the iterative process is started, and (3) the departure of the initial guess from the true unknown solution. The most severe convergence problems are often found in dealing with redox problems involving sharp changes in pE (more than ten orders of magnitude). Major ways to overcome convergence problems include: (1) reducing the size of the time increment in some appropriate manner and (2) improving the condition number of the Jacobian matrix. We remind the reader that the condition number of the matrix of a system of equations measures the sensitivity of the solution to modifications on the input data (Atkinson, 1989). If the condition number is too large, the significance of the results (in this case, the changes in concentrations) can be completely lost.

Convergence is very sensitive to the initial estimates of concentrations. At a given time step, initial concentrations are taken equal to those computed at the previous time step. For the first time step the initial guess is taken from the initial concentrations, which in some cases may deviate largely from the true solution. In these cases, a large number of iterations may be required. For severely non-linear problems the iterative process may fail to reach convergence. Convergence depends strongly upon the case and the nature of chemical reactions. A reasonable time increment is also case-dependent. Before performing the complete simulation, a few trial runs (for a short time period) are suggested to determine the appropriate time increments. Time steps can be increased gradually up to a maximum value when approaching steady-state conditions.

In some cases, concentrations of some species may vary tens of orders of magnitude. For instance, sulfate and bisulfide (SO_4^{2-} and HS^-) concentrations may exhibit extremely large variations between oxidizing and reducing conditions. This may lead to ill-conditioned Jacobian matrices and convergence failures. Basis switching, where most abundant species are dynamically switched as the set of basis species, can greatly improve the condition number of the Jacobian and help to overcome convergence problems (Wolery, 1992; Steefel and Lasaga, 1994). However, much more programming work and computing time is required if basis switching is to be tested everywhere and at all times.

5. Verification

Code verification is a process in which one checks that the code solves properly the equations it is

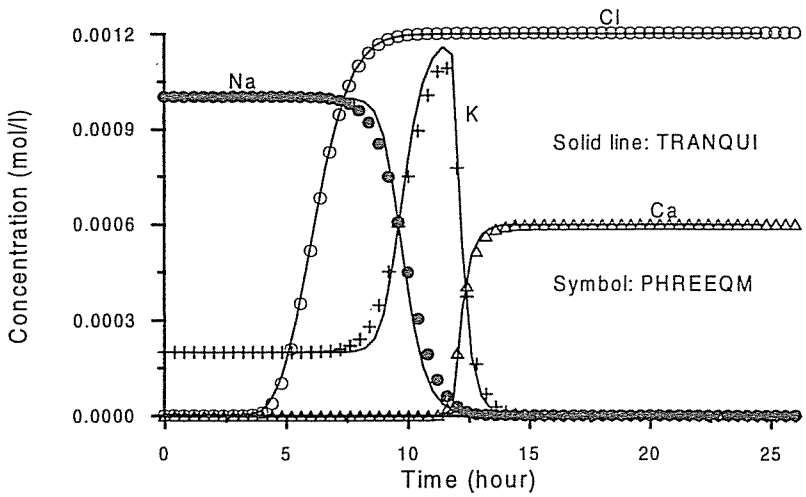

Fig. 1. Example of TRANQUI verification for cation exchange. Concentration breakthrough curves computed with TRANQUI (solid lines) and PHREEQM (symbols) at $x = 0.062$ m.

intended to solve. TRANQUI was verified against available analytical solutions for water flow, heat and solute transport. TRANQUI verification examples are described byXu et al. (1995). Verification of reactive transport was performed by comparison with other reactive transport codes such as PHREEQM (Nienhuis et al., 1991) for cation exchange and UNSATCHEM-2D (Šimnek and Suarez, 1994) for reactive transport in variably saturated media. In other cases TRANQUI was verified using published test cases. Adsorption was verified using a test example modeled with TRANQL (Cederberg et al., 1985) while redox and mineral dissolution/precipitation was verified with DYNAMIX (Liu and Narasimhan, 1989). Here we only report the cation exchange verification test, which corresponds to a laboratory column documented in the PHREEQM User's manual (Nienhuis et al., 1991). The column is initially filled with porewaters containing 1 mM of $NaNO_3$ and 0.2 mM of KNO_3. The column is flushed at a constant discharge of 0.072 m/day with a 0.6 mM $CaCl_2$ solution. Its length is 0.1 m and the porous material has a porosity of 0.3, a dispersivity of 0.0001 m, and a cation exchange capacity (CEC) of 0.01779 meq/100 g. The density of the solids is equal to 2650 kg/m^3. The effect of molecular diffusion is considered negligible. Redox reactions, which could affect nitrate concentrations, are disregarded. Therefore, both nitrate and chloride are considered as conservative species. All thermodynamic data used in TRANQUI are the same as those of the PHREEQM. Sodium is used as the reference cation. The selectivity coefficients of other cations, K^+ and Ca^{2+}, with respect to Na^+ are $K_{NaK} = 0.1995$ and $K_{NaCa} = 0.3981$, respectively.

Computed breakthrough curves at a point located 0.062 m downstream the column inlet are shown in Fig. 1. Numerical results obtained with both codes agree for the most part. Numerical solutions for a conservative ion (Cl^-) coincide entirely. There are some minor differences in the potassium curve which, according to Xu (1996), are because of the differences in the numerical algorithms used by the two codes. In fact, these differences tend to decrease as dispersivity decreases. Fig. 1 illustrates clearly that the incoming solution, which is rich in Ca^{2+}, displaces the initial solution, which has twice as much Na^+ as K^+. Dissolved potassium has a tendency to displace the exchanged sodium. This is the reason why the curve of dissolved sodium breaks through first. Once all the sodium was leached, calcium exchanges with potassium. This explains the peak of the K^+ breakthrough curve. Once all the potassium is leached, calcium breaks through.

Table 1
Summary of relative differences in computed concentrations with sequential non-iterative (SNIA) and sequential iterative (SIA) approaches for four test cases

Test case	Type of chemical processes	δ_{max} (%) (see Eq. 18(a))	(see Eq. 18(b))
Dissolution	Gypsum dissolution	0.272	0.124
Redox	Pyrite oxidation	0.846	0.214
Adsorption	Cadmium sorption	1.158	0.392
Exchange	See the verification test case presented in this paper	57.4	2.4

6. Comparison of solution approaches (SIA and SNIA)

Some investigators like Walter et al. (1994) claim that physical transport and chemical reaction processes taking place under local equilibrium conditions can be effectively decoupled and therefore solved separately in a sequential manner without the need to iterate between the transport and chemical equations. In order to explore under what conditions this statement holds true, here we report a comparison of the results obtained with two sequential iteration approaches: iterative (SIA) and non-iterative (SNIA). They are compared in terms of relative differences, which are computed as the absolute value of the difference between both solutions divided by their arithmetic average

$$\delta_{ijk} = \frac{|C_{ijk}^{SNIA} - C_{ijk}^{SIA}|}{(C_{ijk}^{SNIA} + C_{ijk}^{SIA})/2}, \tag{17}$$

where C is total dissolved concentration and δ_{ijk} is the relative difference at the ith node for the jth component at the kth time step. Supercripts SNIA and SIA refer to the two approaches being compared. To better summarize the comparison of SIA and SNIA, for each test case we compute both the maximum and the averages of δ_{ijk}, δ_{max} and $\bar{\delta}$

$$\delta_{max} = \max_{\text{all } i,j,\text{and}k} (\delta_{ijk}), \tag{18a}$$

$$\bar{\delta} = \frac{\sum_{i=1}^{N_n} \sum_{j=1}^{N_c} \sum_{k=1}^{N_t} \delta_{ijk}}{N_n N_c N_t}, \tag{18b}$$

where N_n, N_c, and N_t are the number of nodes, chemical components and time steps, respectively.

A first set of SIA and SNIA comparisons were performed by using the same test cases utilized for TRANQUI verification (Xu et al., 1995; Xu, 1996). These are four simple 1-D steady-state flow test cases each one containing a different chemical process. The first case involves gypsum dissolution. The second deals with pyrite oxidation. The third is the cation exchange verification example described above. The fourth case, which coincides with case 2 of Cederberg et al. (1985), involves cadmium sorption in a column. The stability of the numerical solution of the solute transport equation as well as the overall convergence of the iterative procedures are controlled by two dimensionless numbers. The first one is the Peclet number, P, which is defined as the ratio between advective and dispersive transport. Whenever

Table 2
Comparison of CPU times (min in a VAX/4300 computer) required by the sequential iterative (SIA) and the sequential non-iterative (SNIA) approaches

Test	CPU time for the SIA			CPU time for the SNIA		
Case	Transport	Chemistry	Total	Transport	Chemistry	Total
Dissolution	0.12	4.6	4.72	0.11	1.7	1.81
Redox	0.017	0.81	0.827	0.014	0.57	0.584
Adsorption	0.189	10.3	10.489	0.091	4.46	4.551
Exchange	1.68	63.7	65.38	0.73	16.53	17.26

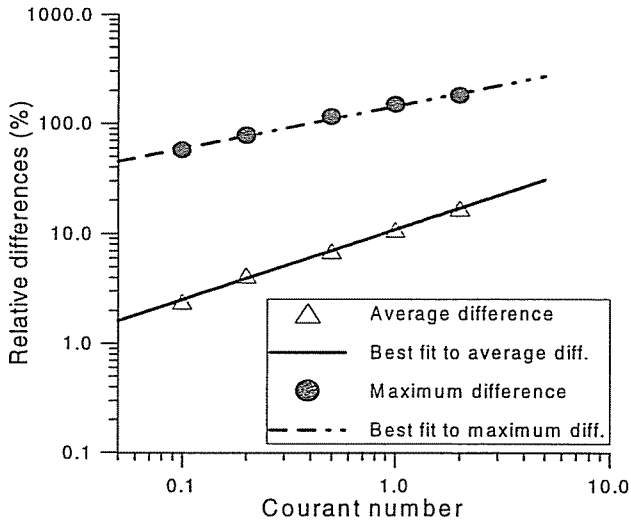

Fig. 2. Log-log plot of maximum and average relative differences in the concentrations computed with SNIA and SIA as a function of the Courant number for the cation exchange verification case. Also shown are the best power fit to each set of data which exponents of 0.64 for average differences and 0.4 for maximum differences.

diffusion is negligible, the grid Peclet number is equal to $\Delta x/\alpha$, where Δx is the grid or cell size and α is dispersivity. Stability is ensured if $P < 2$. The second dimensionless number is the Courant number, C, which is defined as $v\Delta t/\Delta x$ where v is water velocity and Δt is time increment. In order to ensure stability C must be less than 1, although usually $C < 1/3$.

A Peclet number of 1 and a Courant number of 0.1 were used in all four cases. Table 1 summarizes the maximum and average relative differences. For cases involving dissolution, redox and adsorption the maximum relative difference is always less than 1.16% while the average difference is below 0.4%. The largest differences are observed in the test case involving cation exchange. Here the maximum relative difference amounts to 57.4% while the average difference is equal to 2.4%. The comparison of the two approaches in terms of computing time is summarized in Table 2. It can be seen that the SIA requires from 2–4 times more CPU time than the SNIA. It should be noticed that most of the computing time is taken by chemical calculations (see Table 2). This confirms the assessments of Yeh and Tripathi (1991).

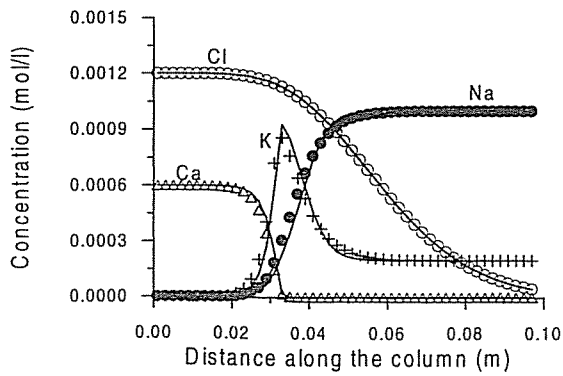

Fig. 3. Spatial distribution of computed concentrations after 6 h with SNIA (symbols) and SIA (lines) using Courant and Peclet numbers equal to 1 for the cation exchange verification case.

To evaluate the effect of increasing the Courant number, additional runs were performed for the following Courant numbers: 0.1, 0.2, 0.5, 1.0 and 2.0 while keeping constant the Peclet number. Both the maximum and average differences increase with increasing Courant number. Fig. 2 shows a log–log plot of average and maximum relative differences. Both sets of data fit quite well to straight lines, which have slopes of 0.64 for average differences and 0.4 for maximum differences. Notice that the average difference has a small value (2.4%) for $C = 0.1$, but reaches a significant amount (17.2%) for $C = 2$. Maximum relative differences are much greater and vary from 57.4% for $C = 0.1$ to 184% for $C = 2$.

Table 3
Relative differences in concentrations computed with sequential non-iterative (SNIA) and sequential iterative (SIA) approaches and CPU time requirements (min in a VAX/4300 computer) for different values of Peclet and Courant numbers corresponding to the Llobregat Delta aquitard example in Section 7

Peclet and Courant numbers		Relative difference		CPU time	
Peclet	Courant	Maximum (%)	Average (%)	SNIA	SIA
0.5	0.0579	16.32	1.32	19.14	36.17
0.5	0.2316	37.02	1.38	5.79	15.15
0.5	0.4632	56.68	1.90	3.28	9.97
0.5	0.9264	85.72	3.38	2.32	7.67
1.0	0.0579	17.48	1.36	20.73	38.82
1.0	0.2316	39.52	1.52	5.65	15.18
1.0	0.4632	57.86	2.74	3.61	10.10
1.0	0.9264	96.04	4.66	2.43	6.17
2.0	0.0579	19.28	1.42	19.85	42.18
2.0	0.2316	58.88	1.78	5.84	14.72
2.0	0.4632	92.08	3.04	3.67	10.27
2.0	0.9264	123.0	5.00	2.32	8.23

Fig. 3 shows the spatial distribution of concentrations as computed with SNIA and SIA with Courant and Peclet numbers equal to 1. The differences between the two approaches take place near the moving concentration fronts (turning points in Fig. 3) where the concentrations of incoming waters differ significantly from initial concentrations. The maximum difference δ_{max} is equal to 131.2% and takes place downstream of the Ca front where Ca concentrations are close to zero. There are noticeable differences in the potassium curves. The curve computed with SNIA is smoother than that of SIA. indicating that SNIA introduces more numerical dispersion. This result is consistent with the findings of Herzer and Kinzelbach (1989) who concluded from both theoretical and numerical analyses that decoupling of transport and chemical equations introduces always numerical dispersion unless these equations are solved iteratively. This smearing effect of SNIA is also shown in the Ca curve. As expected. both approaches provide the same numerical solution for Cl because it is a conservative species that is only subject to tranport.

The accuracy of SNIA as a function of space and time discretization was analyzed using a more complex problem of reactive transport through the Llobregat Delta aquitard, which is described, in Section 7. A variety of Peclet and Courant numbers are used for both approaches (SNIA and SIA). This real case study involves the following chemical processes: cation exchange, calcite dissolution and redox. Table 3 shows both the maximum and average relative differences as well as the CPU time requirements. Numerical differences between both approaches depend strongly on the Courant number and follow a similar trend to that shown in Fig. 2. The Peclet number also affects the magnitude of the differences, although its effect is much smaller than that of Courant number. For the smallest P and C values ($P = 0.5$ and $C = 0.0579$) the average difference is rather small (1.32%) while the maximum difference is equal to 16.32%. For the largest P and C values ($P = 2$ and $C = 0.9264$), the average difference takes a small but significant value of 5% whereas the maximum difference amounts to 123%. In general, the CPU time for SNIA is less than half of that required for SIA. One should notice the dramatic increase in CPU time for both approaches when the Courant number is decreased.

The results of the previous test cases allow us to draw the following conclusions about SIA and SNIA.

(1) SNIA is numerically more efficient than SIA. In our test examples, SNIA requires from 2–3 times less CPU time as than SIA.

(2) Numerical solutions obtained with SNIA, however, are less accurate than SIA solutions and contain more numerical dispersion. The accuracy

of SNIA depends on: a) the grid Peclet and Courant numbers, the latter having a stronger effect; and b) the type of chemical process. The largest errors are found in problems involving cation exchange. This is a striking result for which we cannot provide a rigorous proof. A plausible explanation for cation exchange processes causing the largest errors is related to the highly non-linearity of these processes. We recall that according to Eq. (8) all exchange reactions are coupled in a non-linear manner. The non-linearity is especially acute when a divalent cation exchanges with a monovalent cation.

(3) For sufficiently small Peclet and Courant numbers (i.e., satisfying the stability conditions) the average relative difference between SNIA and SIA are generally small. The maximum relative differences, however, may be rather large locally.

(4) For large Peclet and Courant numbers (i.e., above the stability requirements) the average errors of SNIA may be significant (on the order of 15%). The maximum error can be as large as 184%.

(5) In summary, the question of whether chemical reaction terms can effectively be decoupled from the transport equations depends on time and space discretization parameters, the nature of the chemical reactions involved, and the desired and acceptable accuracy.

7. Field application: Chemical evolution through the Llobregat Delta aquitard

A field study dealing with cation chromatographic separation through a vertical column of the Llobregat River Delta aquitard (Barcelona, Spain) was simulated with TRANQUI. This problem wás risen by Custodio et al. (1971) and originally investigated by Peláez (1983). Later, Manzano (1993) conducted a more in-depth study and more recently Manzano and Custodio (1995), (1998) have presented detailed discussions. All data used here are basically taken from Manzano (1993). The regional setting of this two-layer aquifer separated by the aquitard here considered is described elsewhere (Custodio et al.. 1971; Iribar and Custodio, 1992).

The cation content of interstitial water in the Llobregat Delta aquitard shows the typical distribution of saline water in equilibrium with the soil, which is being displaced by upwards fresh water flow. Manzano (1993) used PHREEQM to evaluate the effects of the mixing of local marine water (which was considered representative of original marine connate water when the aquitard was deposited) and fresh water flowing upwards from the deep aquifer. In her numerical model, she accounted for the simultaneous effect of hydrological transport, cation exchange and calcite dissolution–precipitation. Computed dissolved cation concentrations were compared to available data derived from undisturbed aquitard samples.

Extending previous works, here we analyze: (a) the sensitivities of dissolved and exchanged cation concentrations to changes in selectivity coefficients and (b) the effect of accounting for oxidation–reduction processes (considering the redox pair: $CH_4(aq)/HCO_3$) in addition to aqueous complexation, cation exchange and calcite dissolution.

7.1. Hydrogeological and geochemical system

The 35 m thick saturated aquitard column, constituted by a clay–silt layer, and is homogeneous in terms of hydrological properties. The main hydrodynamic parameters were calibrated by Manzano (1993) from 1-D conservative transport of chloride along the aquitard column based on observed concentrations and known ranges of hydrological parameters. Porosity is equal to 0.411, longitudinal dispersivity amounts to 0.7 m while the diffusion coefficient takes a value of 3.2×10^{-3} m^2/year. The steady-state Darcy velocity is equal to 2.373×10^{-3} m/year. These values are coherent with those found by Peláez (1983) in other boreholes of the same study area. Based on sedimentological considerations and geochemical evidence, it can be assumed that the aquitard was initially filled with marine water (Manzano, 1993). The fresh water comes from a deep aquifer, which is considered as the bottom boundary. The deep aquifer was flushed from original saline water in the study area because it is open to the sea bottom and has a high enough freshwater head to maintain a significant groundwater discharge into the sea. It is believed that the Llobregat River Delta aquifer system was in close to steady-state head conditions during the last 3500 years. Data from the beginning of this century, before major aquifer

Table 4
Total dissolved component concentrations (mmol/l) of initial and bottom boundary water solutions (according to Manzano, 1993)

Component	Initial	Boundary
CL	613.17	5.01
C	32.0	32.0
S	8.5	0.4
Na	521.9	51.67
K	12.82	2.74
Ca	5.0	1.8
Mg	32.6	3.0
N	15	0.9
Ph	7.9	6.83
Pe	− 5	0.0

development, showed a freshwater head at the lower aquitard boundary of circa + 6 m above mean sea level and + 1 m at the upper boundary. The effect of recent intensive development of groundwater from the deep aquifer is described elsewhere and its effect on the aquitard water column is described in Manzano (1993).

Table 5
List of geochemical reactions and processes considered in the Llobregat Delta aquitard reactive transport model. Here "-X" denotes a cation exchange site

Geochemical reactions	$\log_{10}$ (K) at 25°C
Aqueous dissociation:	
$OH^- = H_2O - H^+$	13.995
$CO_3^{2-} = HCO_3^- - H^+$	10.329
CO_2 (aq) $= HCO_3^- + H^+ - H_2O$	− 6.3447
$CaHCO_3^+ = Ca^{2+} + HCO_3^-$	− 1.0467
$MgHCO_3^+ = Mg^{2+} + HCO_3^-$	− 1.0357
$CaCO_3$ (aq) $= Ca^{2+} + HCO_3^- - H^+$	7.0017
$MgCO_3$ (aq) $= Mg^{2+} + HCO_3^- - H^+$	7.3499
$NaHCO_3$ (aq) $= Na^+ + HCO_3^-$	− 0.1541
$CaSO_4$ (aq) $= Ca^{2+} + SO_4^{2-}$	− 2.1111
$MgSO_4$ (aq) $= Mg^{2+} + SO_4^{2-}$	− 2.309
$NaSO_4^- = Na^+ + SO_4^{2-}$	− 0.82
$KSO_4^- = K^+ + SO_4^{2-}$	− 0.8796
Oxidation–reduction:	
CH_4 (aq) $= HCO_3^- - 3H_2O + 9H^+ + 8e^-$	− 27.655
Cation exchange:	
$Na^+ + 0.5Ca\text{-}X_2 = 0.5Ca^{2+} + Na\text{-}X$	See Table 7
$Na^+ + 0.5Mg\text{-}X_2 = 0.5Mg^{2+} + Na\text{-}X$	See Table 7
$Na^+ + K\text{-}X = K^+ + Na\text{-}X$	See Table 7
$Na^+ + NH_4\text{-}X = NH_4^+ + Na\text{-}X$	See Table 7
Mineral dissolution − precipitation:	
$CaCO_3$(s) (Calcite) $= Ca^{2+} + HCO_3^- - H^+$	1.8487

Table 6
Cation selectivity coefficients (according to Gaines-Thomas convention) and CEC values inferred from experimental data obtained by Manzano (1993). The medium has a bulk density of 1.75 kg/l. $K_{Na\ cation}$ denotes the cation selectivity with respect to Na^+

Depth (m from top of the aquitard)	$K_{Na\ K}$	$K_{Na\ Ca}$	$K_{Na\ Mg}$	CEC (meq/100 g)
1	0.1217	0.2979	0.2606	14.16
5	0.1743	0.2541	0.4645	15.0
21	0.1684	0.2570	4.2106	15.0
33	0.0787	0.0649	0.0698	17.0

The initial concentrations (see Table 4) are taken from available data on chemical composition of pore-waters extracted from undisturbed samples in the upper part of the aquitard column. These data almost coincide with the chemical composition of present Mediterranean sea water. The lower boundary concentrations adopted in the numerical model were taken from available chemical data in the lowermost part of the aquitard where the native saline water has already been leached. The list of chemical reactions and processes considered in TRANQUI numerical simulations are listed in Table 5. All these processes are assumed to occur under local equilibrium conditions.

Two sets of runs were performed. The first set includes four runs in which aqueous complexation, cation exchange and calcite dissolution–precipitation were considered. These runs were performed to analyze the sensitivity of dissolved and exchanged cation concentrations to cation selectivity coefficients. Cation exchange was formulated using the Gaines–Thomas convention (see Appelo and Postma, 1993), according to which the activities of exchanged cations are equal to their equivalent fractions.

It should be pointed out that selectivity is a relative concept. Na^+ is chosen as the reference cation, and therefore its selectivity is equal to one. According to this definition and the cation exchange formulation (see Table 5), the lower the selectivity the higher the exchange capacity. Divalent cations have stronger affinity for exchange than monovalent cations. Major cations in groundwaters usually obey the following

Table 7
Cation selectivity values used in the first four runs. Underlined are the selectivities that change in each run

Run	K_{NaK}	$K_{Na\,Ca}$	$K_{Na\,Mg}$	$K_{Na\,NH4}$
1	0.1543	0.2697	0.3626	0.5
2	0.4995	0.2697	0.3626	0.5
3	0.1543	0.2697	0.6573	0.5
4	0.1543	0.1581	0.6573	0.5

preference exchange sequence: $Ca^{2} > Mg^{2-} > K^{+} > Na^{+}$ (Appelo, 1994). Manzano (1993) presents measured values of CEC and selectivity coefficients at different depths along the aquitard (see Table 6).

Table 6 shows that measured cation selectivities at a depth of 33 m have extremely low values. Similarly, Mg^{2+} selectivity at a depth of 21 m has an extremely large value of 4.2106. These extreme values were disregarded in the present simulations. For the numerical simulations it was assumed an average CEC value of 15 meq/100 g solid (or 645.3 meq/l solution) for the entire column. Similarly, cation selectivities were assumed constant in the whole aquitard. For the first run, these selectivities were taken equal to the averages of measured values (excluding extreme values). Table 7 summarizes the adopted selectivity coefficients. No measurements were available for the NH_4^+. Its selectivity was assigned an arbitrarily large value (0.5), which prevents a large exchange of NH_4^+. The sensitivities to cation selectivities were *analyzed by modifying the values of* K_{NaK}, K_{NaMg} *and* K_{NaCa} one at a time (see runs 2–4 in Table 7).

7.2. Results

7.2.1. Selectivity runs

Fresh water coming from the deep aquifer mixes with saline water and causes a noticeable dilution. This is clearly shown by concentration data Cl^-, Na^+, Ca^{2+}, Mg^{2+}, and K^+, which are shown in Figs. 4 and 5. These figures also include the corresponding computed concentrations after 800, 1600, 3200 and 4800 years. As a result of dilution, calcite dissolves (see Fig. 6(a)). CO_3^{2-} produced by calcite dissolution associates with H^+ to form HCO_3^-, thus increasing pH (see Fig. 6(b)). After 1600 years, a local maximum pH peak is developed which moves upwards, but at a slower pace than the mean water velocity. At the bottom of the aquitard, pH keeps increasing until 1600 years. After this time, it decreases slightly and approaches the pH of the boundary water.

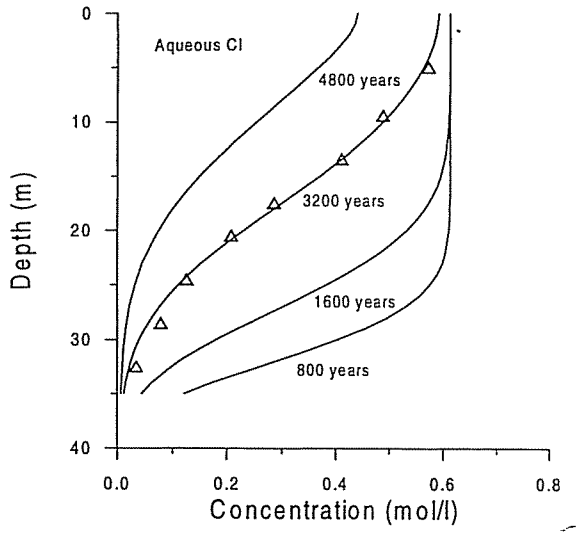

Fig. 4. Measured (symbols) and computed (lines) concentrations of Cl^- at 800, 1600, 3200 and 4800 y.

In the model it is assumed that initial exchange cation concentrations are in equilibrium with the aqueous solution. Most of the exchange sites are initially occupied by Na^+, up to 0.394 mol/l (see Fig. 7(a)), because of the extremely large initial dissolved Na^+ concentration of 0.522 mol/l. The initial exchanged concentrations of Ca^{2+}, Mg^2, K^- and NH_4^+ in the aquitard column are 0.058, 0.022, 0.068 and 0.021 mol/l, respectively. Dilution causes a decrease of Na^+ dissolved concentration which in turn induces the release of Na^+ from the exchange complex. The remaining dissolved cations, Ca^{2+}, Mg^{2+}, K^+ and NH_4^+, take over the exchange sites. Computed concentrations of exchanged Na^+ decrease at the bottom of the aquitard (see Fig. 7(a)) while those of other cations (Ca^{2+}, Mg^2, K^+ and NH_4^+) increase in order to maintain constant the CEC. Exchanged sites released by Na^+ are occupied mainly by Ca^{2+} because of its high exchange capacity. As shown in Fig. 7(b), exchanged Ca^{2+} shows a maximum value of 0.2 mol/l at the bottom of the aquitard after 4800 years.

By comparing the spatial distribution of dissolved and exchanged concentrations for Na^+ (see Figs. 5(a) and 7(a)) and Ca^{2+} (see Figs. 5(b) and 7(b)) one can

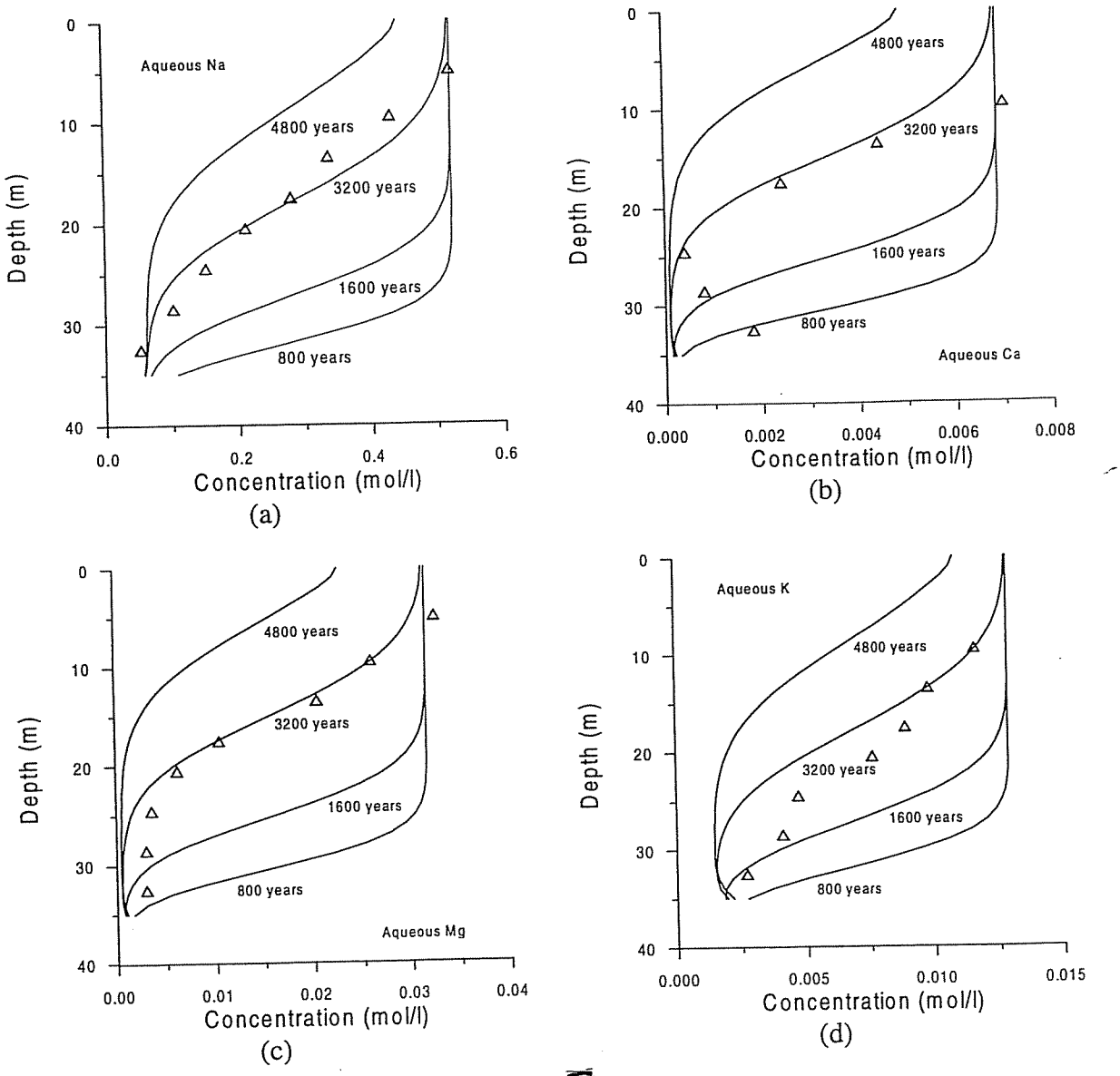

Fig. 5. Measured dissolved Na^+ (a), Ca^{2-} (b), Mg^{2-} (c) and K^+ (d) concentrations (symbols) and computed values (lines) at 800, 1600, 3200 and 4800 y corresponding to run 1 of TRANQUI.

see that the fronts of exchanged concentrations are steeper than those of aqueous concentrations. In addition, the former show a noticeable retardation caused by cation exchange.

The simulated concentrations of conservative Cl^- after 3200 years match fairly well the measured values. Computed concentrations of dissolved cations also show a good fit to the available data, although there are some discrepancies in the Ca^{2-}, Mg^{2-} and K^- curves, especially near the bottom boundary. These results coincide for the most part with those obtained by Manzano (1993) using the PHREEQM code.

The results obtained by changing cation selectivities (runs 2–4) indicate that exchanged cation

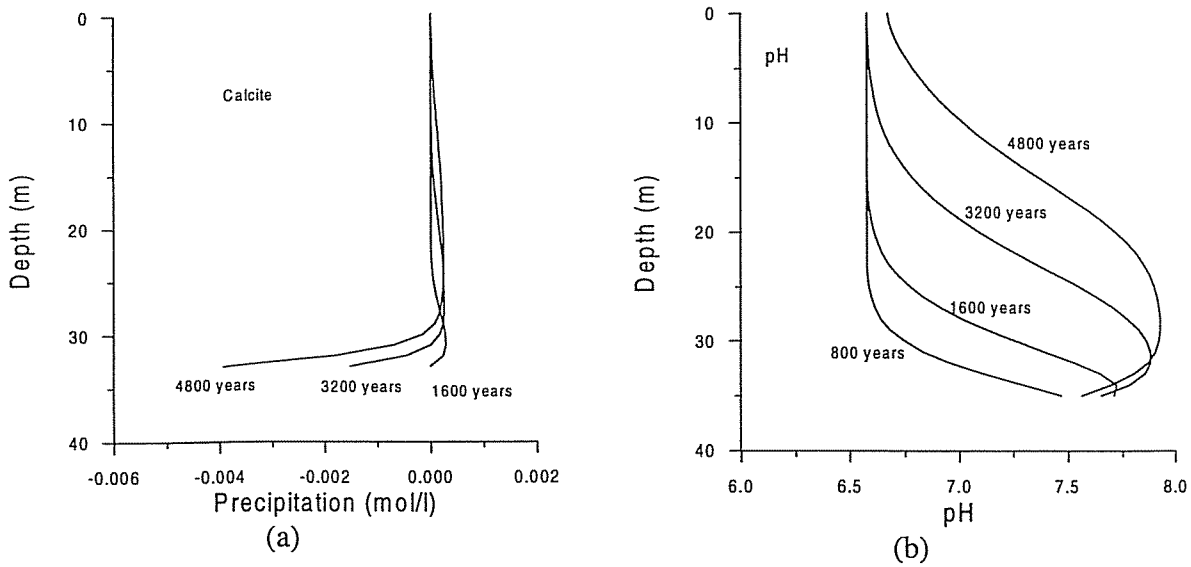

Fig. 6. Total cumulative calcite precipitation (a, negative values indicate dissolution) and pH (b) distribution after 800, 1600, 3200 and 4800 y corresponding to run 1 of TRANQUI.

concentrations are more sensitive to selectivities than aqueous cations. Changes in cation selectivities result in a redistribution of exchanged cations throughout the entire column which in turn affects slightly the concentrations of aqueous cations. For the purpose of illustrating the sensitivities, here we only report the results of run 2. Additional results can be found in Xu (1996).

When the K^+ selectivity in increased from 0.1543 (run 1) to 0.4995 (run 2), its exchange capacity is

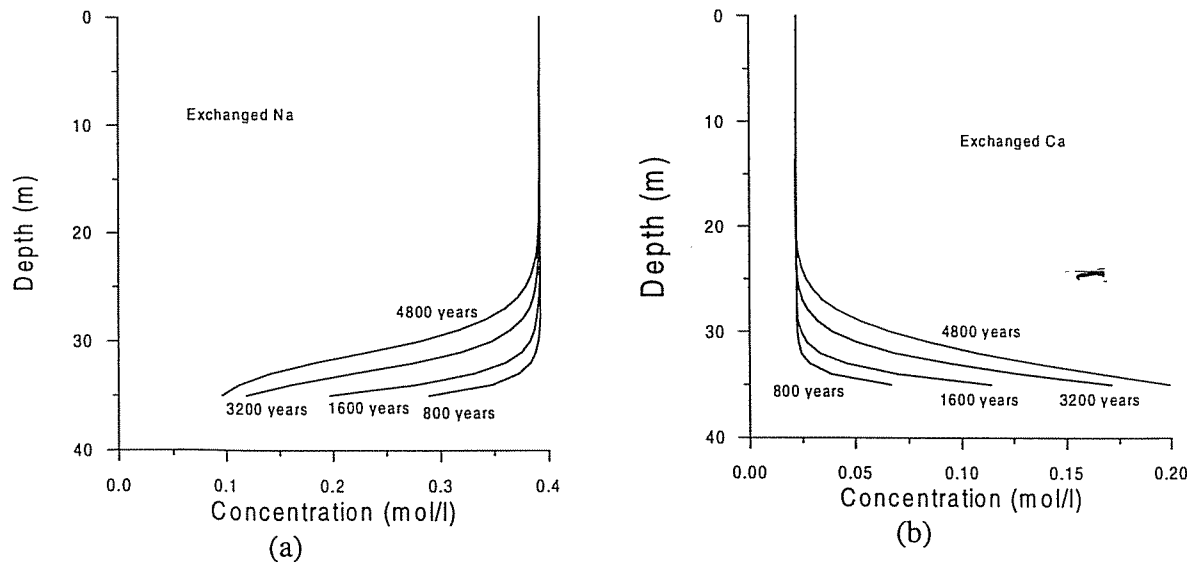

Fig. 7. Exchanged Na^- (a) and Ca^{2-} (b) concentrations at 800, 1600, 3200 and 4800 y corresponding to run 1 of TRANQUI.

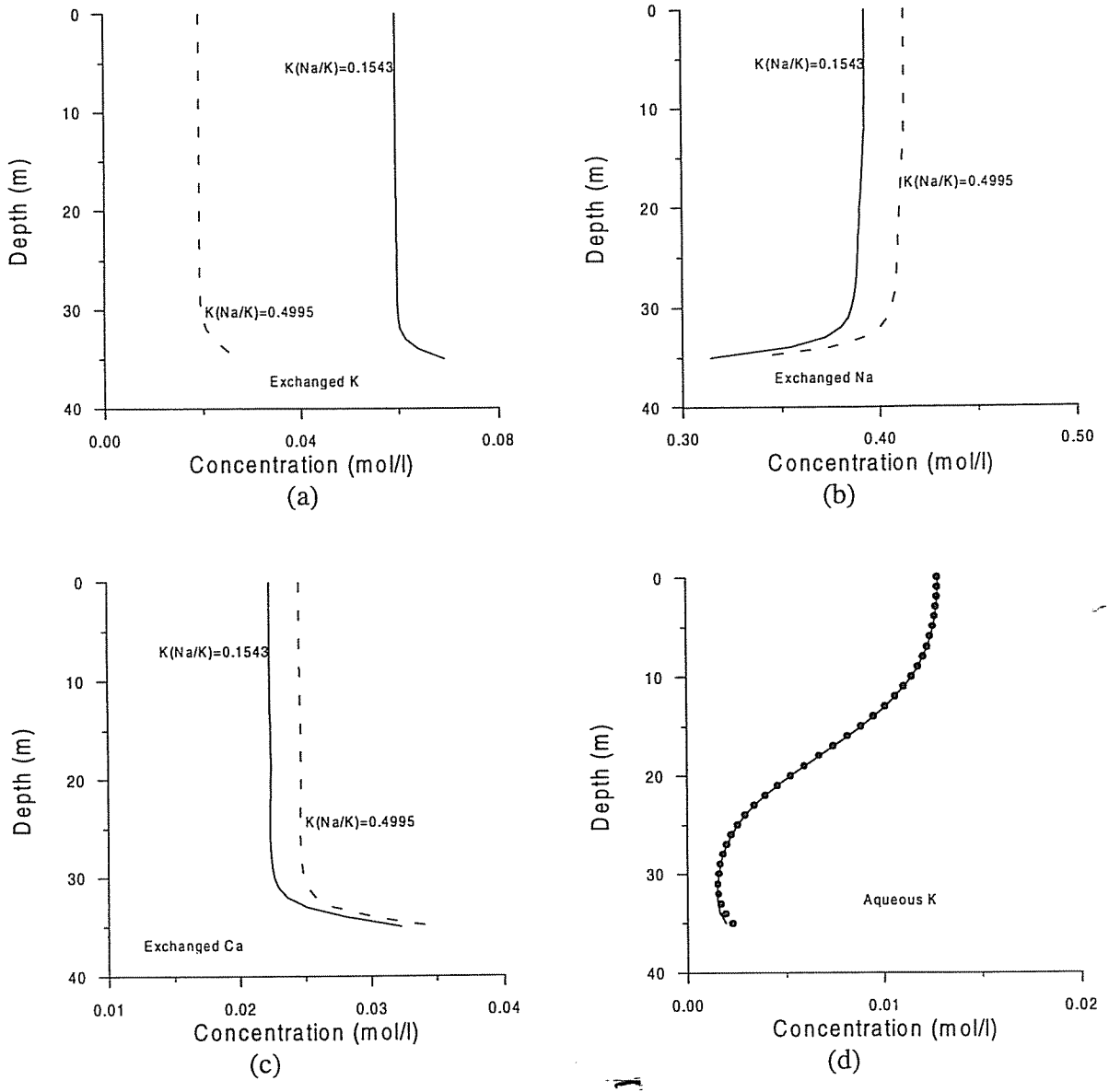

Fig. 8. Exchanged K^+ (a), Na^{2+} (b), Ca^+ (c) and aqueous K^+ (d) concentrations at 3200 y using selectivities $K_{NaK} = 0.1543$ for run 1 (solid lines) and 0.4995 for run 2 (dash lines and symbols).

reduced. The initial exchanged K^+ concentration decreases from 0.06 mol/l in run 1 to 0.0193 mol/l in run 2 (Fig. 8(a)). The exchange sites vacated by K^+ are compensated by the other cations. There is a considerable increase of exchanged Na^+, Mg^{2+}, and NH_4^+ (only Na^+ and Ca^{2+} are presented in Figs. 8(b) and (c)). However, aqueous K^+ concentrations computed with the two selectivities are almost identical, with very mild differences near the bottom boundary (Fig. 8(d)). The same trend is observed for the rest of dissolved cations.

7.2.2. *Redox runs*

A second set of four runs were carried out taking

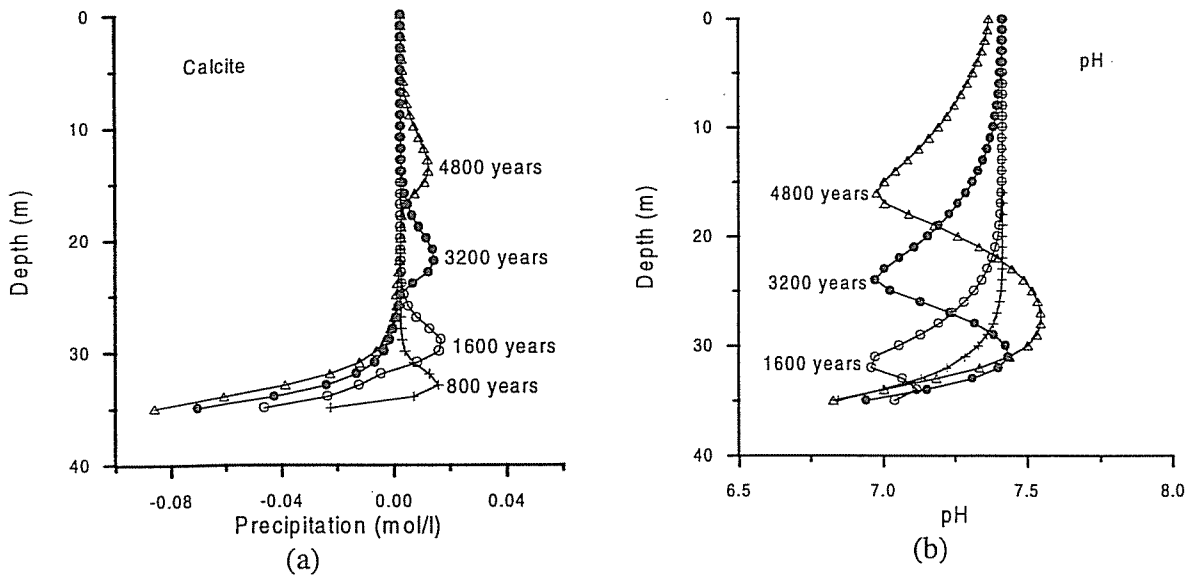

Fig. 9. Total cumulative calcite precipitation (a), negative values indicate dissolution) and pH (b) distribution obtained with run 5 (initial pE = 5 and bottom boundary pE = 0) after 800, 1600, 3200 and 4800 y.

into account oxidation-reduction reactions in addition to cation exchange and calcite dissolution reactions. Although no redox data were available, experimental evidence indicates that native aquitard porewaters have reducing conditions with methane-production in the lower part (Manzano, 1993). Several combinations of initial and boundary pE values were tested and the best set of values are those listed in Table 4. Redox reactions exert a great effect on pH which in turn controls the amount of calcite dissolution/precipitation and consequently the concentration of aqueous calcium.

When redox processes are considered, the initial pH is equal to 7.4, which is greater than the initial pH of run 1 (pH = 6.6) (compare Figs. 9(b) and 6(b)). The mixing of fresh oxidizing water and native reducing aquitard water triggers both redox and dissolution processes. The incoming fresh water causes a dilution effect, which induces calcite dissolution and pH increase as already mentioned previously. Simultaneously, the oxidizing nature of incoming water increases pE what in turn causes the transformation of CH_4 (aq) into HCO_3^-. Consumption of 1 mol of CH_4 (aq) produces 9 mole of H^+. Therefore, the mixing of oxidizing water with native water causes a significant decrease in pH. Notice that the oxidation of CH_4 (aq) and the dissolution of calcite cause opposite effects on pH. While CH_4 (aq) oxidation induces a pH decrease, the pH increases when dissolves. Computed pH values at the bottom of the aquitard show first a decreasing trend associated to CH_4 (aq) oxidation (Fig. 9(b)). The oxidation also induces calcite precipitation (see Fig. 9(a)). Once the effect of oxidation attains a steady state, calcite dissolution takes over and pH starts increasing. These two opposite trends are clearly shown in the pH and calcite plots (Fig. 9). A minimum pH peak value is developed after 1600 years. The pH minimum moves slightly slower than average porewater velocity. After 4800 years is located at a depth of 15 m. Behind the pH minimum peaks, there are pH maximum peaks associated to calcite dissolution (see Fig. 9).

Redox and dissolution reactions have a clear effect on the concentration of aqueous cations. Total aqueous concentrations of Na^+, Ca^{2+}, Mg^{2+}, and K^+ are presented in Fig.10(a),(b),(c)and(d). Computed values of aqueous Na^+, Ca^{2+}, and Mg^{2+} match their corresponding measured data much better than in run 1 (compare Figs. 5 and 10), especially near the bottom boundary. Computed

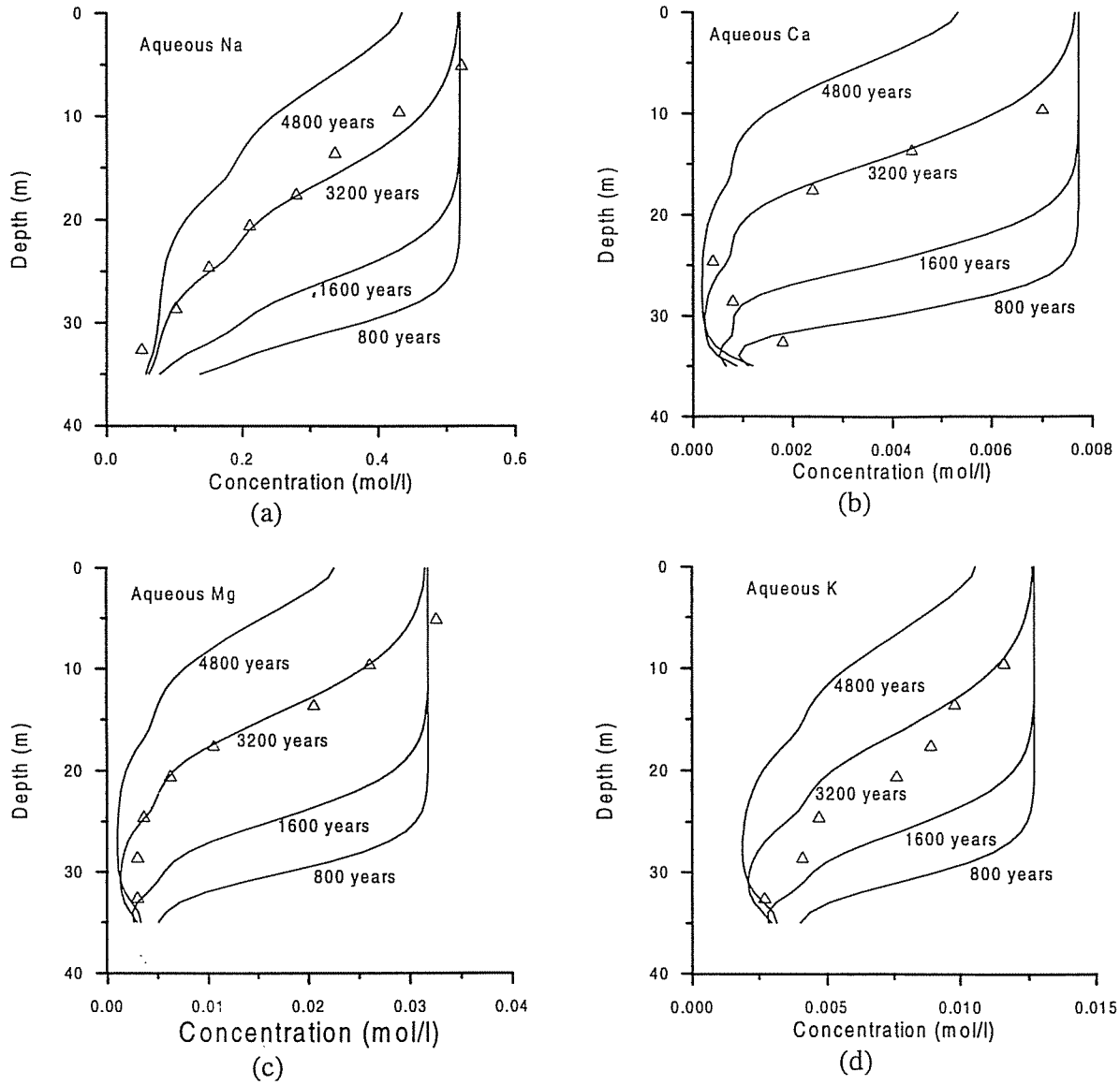

Fig. 10. Measured aqueous Na^- (a), Ca^{2+} (b), Mg^{2+} (c) and K^+ (d) concentrations (symbols) and computed values (lines) at 800, 1600, 3200 and 4800 y corresponding to run 5 of TRANQUI.

concentrations of aqueous K^+ show only a slight improvement compared to run 1 (compare Figs. 5(d) and 10(d)).

8. Conclusions

A general 2-D finite element reactive solute transport code, TRANQUI, was developed using a sequential iteration approach. General water flow, solute and heat transport conditions are considered for fully or partly saturated media. The code accounts for hydrological, thermal and a wide range of chemical processes such as aqueous complexation, acid–base and redox reactions, mineral dissolution/precipitation, gas dissolution/ex-solution, ion exchange and

adsorption. TRANQUI relies on modified versions of EQ 3/6 databases. In addition to the fully iterative sequential approach (SIA), a sequential non-iterative approach (SNIA), in which transport and chemistry are de-coupled, was implemented and tested. The accuracy and numerical efficiency of SIA and SNIA were systematically analyzed using several test cases from which we draw the following conclusions:

1. SNIA is numerically more efficient than SIA. In our test examples, SNIA requires about half CPU time of SIA.
2. Numerical solutions obtained with SNIA, however, are less accurate than SIA solutions and contain more numerical dispersion. The accuracy of SNIA depends on: (a) the grid Peclet and Courant numbers, the latter having a stronger effect; and (b) the type of chemical process. The largest errors are found in problems involving cation exchange. A plausible explanation for cation exchange processes causing the largest errors is related to the high non-linearity of these processes, especially acute when a divalent cation exchanges with a monovalent cation.
3. For sufficiently small Peclet and Courant numbers (i.e., satisfying the stability conditions) the average relative difference between SNIA and SIA are generally small. The maximum relative differences, however, may be large locally.
4. For large Peclet and Courant numbers (i.e., above the stability requirements) the average errors of SNIA may be significant (on the order of 15%). The maximum error can be as large as 184%.

Therefore, there is no conclusive answer to the question of whether chemical reaction terms can be effectively de-coupled from the transport equations. In general, this decoupling will be acceptable depending on time and space discretization parameters, the nature of chemical reactions and the desired accuracy.

A field study dealing with cation chromatographic separation through a vertical column of the Llobregat River Delta aquitard near Barcelona (Spain) was modeled with TRANQUI. The main conclusions of the reactive solute transport modeling in the Llobregat Delta aquitard are:

1. Exchanged cation concentrations are found to be much more sensitive to changes in cation selectivities than the concentrations of dissolved cations.
2. Redox processes affect the transport of reactive cations by means of a pronounced decrease in pH. Accounting for redox processes leads to a significant improvement of the fit of aqueous Ca^{2+}, Mg^{2-} and Na^{+} concentrations.
3. The ability of TRANQUI to account for a wide range of chemical processes and reproduce reasonably well the observed concentrations in the Llobregat Delta aquitard is taken as an indication of partial validation in the sense that the code is a tool that can be safely applied to modeling complex natural hydrogeochemical systems

Acknowledgements

The work presented was carried out within the framework of R and D projects funded by the Spanish Agency for Nuclear Waste Disposal, ENRESA, and the Commission of the European Community (Program RADWAS, contracts FI2W-CT91-0102, FI4W-CT95-0008 and FI4W-CT95-0006). We are grateful to Jordi Delgado and Nuria Cuéllar for their help in processing the hydrochemical data of the Llobregat Delta aquitard. Thanks are also given to Steve White for a careful review of the manuscript and constructive suggestions. We appreciate the valuable comments and suggestions of the two anonymous reviewers, which have significantly improved the final version of the article.

References

Atkinson, K., 1989 An Introduction To Numerical Analysis. Wiley, New Jersey. 573 pp.

Appelo, C.A.J., 1994. Cation and proton exchange, pH variations and carbonate reactions in a freshening aquifer. Water Resour. Res. 30 (10). 2793–2805.

Appelo, C.A.J., Postma, D., 1993 Geochemistry, Groundwater and Pollution. Balkema, Rotterdam, 536 pp.

Bear, J., 1979 Hydraulics of Groundwate. McGraw-Hill, New York, 569 pp.

Carnahan, C.L., 1990 Coupling of precipitation/dissolution reactions and mass diffusion via porosity changes. In: Melchior, D.C. Bassett, R.L. (Eds.), Chemical Modeling of Aqueous Systems II, American Chemical Society, Washington, DC, pp. 234–242.

Cederberg, G.A., Street, R., Leckie, J.O. A groundwater mass transport, 1985. equilibrium chemistry model for multicomponent systems. Water Resour. Res. 21 (8), 1095–1104.

Custodio, E., Bayó, A., Peláez, M.D., 1971 Geoquímica y datación

de aguas para el estudio del movimiento de las aguas subterráneas en el delta del Llobregat (Barcelona). In: I Congreso Hispano-Luso-Americano de Geología Económica, Madrid-Lisbon, vol. 1, pp. 51–90. (in Spanish).

de Marsily, G., 1986 Quantitative Hydrogeology, Acadamic Press, New York, 440 pp.

Engesgaard, P., Kipp, K.L., 1992. A geochemical transport model for redox-controlled movement of mineral fronts in groundwater flow systems: A case of nitrate removal by oxidation of pyrite. Water Resour. Res. 28 (10), 2829–2843.

Galarza, G.A., 1993. Calibración automática de parámetros en problemas no lineales de flujo y transporte, Ph.D. Dissertation, Universidad politécnica de Cataluña, Barcelona, Spain. (in Spanish).

Herzer, J., Kinzelbach, W., 1989. Coupling of transport and chemical processes in numerical transport models. Geoderma 44, 115–127.

Iribar, V., Custodio, E., 1992. Advancement of seawater intrusion in the Llobregat delta aquifer, In: Study and Modeling of Saltwater Intrusion, edited by Centro Internacional de Métodos Numéricos en Ingeniería, Barcelona, Spain, pp. 35–50.

Jennings, A.A., Kirkner, D, 1982. J., Theis, T.L., Multicomponent equilibrium chemistry in groundwater quality models. Water Resour. Res. 18 (4), 1089–1096.

Kirkner, D.J., Theis, T.L., Jennings, A.A., 1984. Multicomponent solute transport with sorption and soluble complexation. Adv. Water Resour. 7, 120–125.

Lensing, H.J., Vogt, M., Herrling, B., 1994. Modeling of biologically mediated redox processes in the subsurface. J. Hydrol. 159, 125–143.

Lichtner, P.C., 1996. Continuum formulation of multicomponent-multiphase reactive transport, In: Reactive transport in porous media. Reviews in Mineralogy, vol. 34, Mineralogical Society of America, pp. 1–79.

Liu, C.W., Narasimhan, T.N., 1989. Redox-controlled multiple species reactive chemical transport, 1. Model development. Water Resour. Res. 25 (5), 869–882.

Manzano, M., 1993. Génesis del agua interstical del acuitardo del delta del Llobregat: origen de los solutos y transporte interactivo con el medio sólido, Ph.D. Dissertation, Universidad Politécnica de Cataluña, Barcelona, Spain. (in Spanish).

Manzano, M., Custodio, E., 1995. Origen de las aguas salobres en sistemas acuíferos deltaicos: applicacion de la teoría de la cromatografía iónica al acuitardo del delta del Llobregat, Hidrogeología y Recursos Hidráulicos, Madrid, vol. XX, pp. 179–201. (in Spanish).

Manzano, M., Custodio, E., 1998. Origen de las aguas salobres en sistemas acuíferos deltaicos: aplicación de la teoría de la-cromatografía iónica al acuitardo del delta del Llobregat, In: IV Congreso Latinoamericano de Hidrología Subterránea, Montevideo (in press). (in Spanish).

Miller, C.W., Benson, L.V., 1983. Simulation of solute transport in a chemically reactive heterogeneous system: Model development and application. Water Resour. Res. 19 (2), 381–391.

Neretnieks, I., Yu, J.W., Liu, J., 1997. An efficient time scaling technique for coupled geochemical and transport models. J. Contam. Hydrology 26, 269–277.

Nienhuis, P., Appelo, C.A.T, Willemsen, A., 1991. Program PHREEQM: Modified from PHREEQE for use in mixing cell flow tube, Free University. Amsterdam, The Netherlands.

Parkhurst, D.L., Thorstenson, D.C., Plummer, L.N., 1980. PHREEQE: A computer program for geochemical calculations, US Geol. Surv. Water Resour. Invest. vols. 80-96, 174 pp.

Peláez, M.D., 1983. Hidrodinámica en formaciones semipermeables a partir de la composición química y radioiotôpica del agua intersticial: aplicación a los limos intermedios del delta del Llobregat, Ph.D. Dissertation,Universidad de Barcelona, Barcelona, Spain. (in Spanish).

Samper, J., Xu, T., Ayora, C., 1994. Modeling groundwater chemical evolution in a closed-basin evaporitic environment, In: Groundwater Quality Mangement. IAHS Pub. 220, pp. 173–182.

Samper, J., Xu, T., Ayora, C., Cuéllar, N., 1995. Reactive solute transport modelling: Numerical formulation and computer codes, Hidrogeología y Recursos Hidráulicos, Madrid, vol. XIX, pp. 785–799.

Šimnek, J., Suarez, D.K., 1994. Two-dimensional transport model for variably saturated porous media with major ion chemistry. Water Resour. Res. 30 (4), 1115–1133.

Steefel, C.I., Lasaga, A.C., 1994. A coupled model for transport of multiple chemical species and kinetic precipitation/dissolution reactions with applications to reactive flow in single phase hydrothermal system. Am. J. Sci. 294, 529–592.

Valocchi, A.J., Street, R.L., Roberts, P.V., 1981. Transport of ion-exchanging solutes in groundwater: Chromatographic theory and field simulation. Water Resour. Res. 17 (5), 1517–1527.

Walsh, M.P., Bryant, S.L., Lake, L.W., 1984. Precipitation and dissolution of solids attending flow through porous media. AIChEJ. 30 (2), 317–328.

Walter, A.L., Frind, E.O., Blowes, D.W., Ptacek, C.J., Molson, J.W., 1994. Modeling of multicomponent reactive transport in groundwater, 1, Model development and evaluation. Water Resour. Res. 30 (11), 3137–3148.

White, S.P., 1995. Multiphase non-isothermal transport of systems of reacting chemicals. Water Resour. Res. 31 (7), 1761–1772.

Wolery, T.J., 1992. EQ3/6: A software package for geochemical modeling of aqueous systems: Package overview and installation guide (version 7.0). Lawrence Livermore National Laboratory, Report UCRL-MA-110662 PT I, California, USA.

Xu, T., 1996. Modeling non-isothermal multicomponent reactive solute transport through variably saturated porous media, Ph.D. Dissertation, University of La Coruña, La Coruña, Spain.

Xu, T., Ayora, C., Samper, J., 1995. Reactive solute transport modelling: one dimensional examples, Hidrogeología y Recursos Hidráulicos. Madrid, vol. XIX, pp. 801–812.

Yeh, G.T., Tripathi, V.S., 1989. A critical evaluation of recent developments of hydrogeochemical transport models of reactive multichemical components Water Resour. Res. 25 (1), 93–108.

Yeh, G.T., Tripathi, V.S., 1991. A model for simulating transport of reactive multispecies components: model development and demonstration Water Resour. Res. 27 (12), 3075–3094.

Zysset, A., 1994. Stauffer. F., Dracos, T., Modeling of chemically reactive groundwater transport. Water Resour. Res. 30 (7), 2217–2228.